

MRI Classification of Parkinson's Disease Using SVM and Texture Features

S. Pazhanirajan and P. Dhanalakshmi

Abstract A novel method for automatic classification of magnetic resonance image (MRI) under categories of normal and Parkinson's disease (PD) is then classified according to the severity of the medical specialty drawbacks. In recent years, with the advancement in all fields, human suffers from numerous specialty disorders like brain disorder, epilepsy, Alzheimer, Parkinson, etc. Parkinson's involves the malfunction and death of significant nerve cells within the brain, known as neurons. As metal progresses, the quantity of Dopastat made within the brain decreases, defeat someone, and make them unable to manage movements commonly. In the planned system, T_2 (spin-spin relaxation time)—weighted MR images are obtained from the potential PD subjects. For categorizing the MRI knowledge, bar graph options and gray level co-occurrence matrix (GLCM) options are extracted. The options obtained are given as input to the SVM classifier that classifies the information into traditional or PD classes. The system shows a satisfactory performance of quite 87 %.

Keywords Electroencephalogram (EEG) · Parkinson's disease (PD) · Gray-level co-occurrence matrix (GLCM) · Support vector machine (SVM)

1 Introduction

Parkinson's disorder (PD) is the second most typical neurodegenerative illness moving several individuals worldwide. A calculable 7 to 10 million individuals worldwide reside with paralysis agitans. Incidence of Parkinson's will increase with

S. Pazhanirajan (✉) · P. Dhanalakshmi
Department of Computer Science and Engineering,
Annamalai University, Chidambaram, India
e-mail: pazhani.sambandam@yahoo.co.in

P. Dhanalakshmi
e-mail: abidhana01@gmail.com

age, however, associate in nursing calculable 4 % of individuals with palladium square measure diagnosed before the age of fifty. The MR image is used to identify spatial map and properties associated with a specific nuclei or proton present in the region being analyzed. The hydrogen proton is the most common form of nuclei used in MRI. These properties are the spin–lattice relaxation time $T1$, spin-spin relaxation time $T2$, and the spin density p . To detect PD, various signals (EEG, speech, etc.) and images (MRI, C.T, etc.) have been undertaken [1].

In [2], of this paper, the authors have proposed a novel technique for automated segmentation of brain structures that are related to PD from low resolution sonographic images. The authors have performed averaging of adjusted spatially varying TCS image as preprocessing step to avoid noise in the image. The segmentation is performed by a tailored shape-based active contour segmentation algorithm.

A novel region of interest (ROI)-based CAD technique using $T1$ -weighted magnetic resonance imaging (MRI) was used to discriminate PD patients from healthy subjects. Features are constructed from gray matter (GM), white matter (WM), and cerebrospinal fluid (CSF) values of voxel from these regions. A decision model is built with the help of support vector machine classifier. The results demonstrate that the proposed method has an accuracy of 86.67 % in identifying PD patients from health subjects [3].

In an expert system proposed in [4], a supervised machine learning approach for identifying sensitive medical image biomarkers which enables automatic diagnosis of individual subjects. Morphological $T1$ -weighted magnetic resonance images (MRIs) of PD patients and PSP patients were analyzed using principal component analysis as feature extraction technique and support vector machine is used for classification.

2 Feature Extraction

2.1 Histogram Processing

The histogram of a digital image with intensity levels in the range $[0, L - 1]$ is a discrete function

$$s(r_k) = \frac{n_k}{n}, 0 \leq k \leq L - 1$$

where r_k is the k th gray level, n_k is the number of pixels in the image with that intensity level, n is the number of pixels in the MRI with $k = 0, 1, 2, \dots, L - 1$. In short, $s(r_k)$ gives an estimate of the probability of occurrence of intensity level r_k [5].

2.2 Histogram Feature Extraction

Histogram equalization is an image enhancement method which uses a monotonically increasing transformation function [6]. The original intensity values r_i are transformed using the function $T(r)$ into new intensity values of the output image as follows:

$$s_i = T(r_i) = \sum_{j=0}^i s_r(r_j) \quad (1)$$

$$\sum_{j=0}^i s_r(r_j) = \sum_{j=0}^i \frac{n_j}{n} \quad \text{for } i = 0, 1, \dots, L - 1 \quad (2)$$

where $S_r(r_i)$ is the probability-based histogram of the input image that is transformed into the output image with the histogram $S_s(s_i)$. The histogram of the input image is stretched using the transformation function $T(r_1)$ in Eq. (2) in such a way that the intensity values in the output image occurs with equal probability of occurrence.

This method achieves uniform distribution by redistributing the intensity values of an image. This methodology could cause saturation in some regions of the image leading to loss of details and high-frequency data which will be necessary for interpretation.

2.3 Texture Feature

The GLCM is created from a grayscale image and hence the values that are checked for co-occurrence are pixels with gray level (grayscale intensity) [7].

2.3.1 Derivation of Texture Features from a Co-occurrence Matrix

In the simplest form, the GLCM $s(a, b)$ is the distribution of the number of occurrences for a pair of gray values a and b separated by a distance vector $d = [dx; dy]$.

We used 22 textural features in our study. The following equations define these features. Let $s(a, b)$ be the (a, b) th entry in a normalized GLCM [8]. we define also

$$s_x(a) = \sum_{b=1}^N s(a, b) \quad (3)$$

$$s_y(i) = \sum_{a=1}^N s(a, b) \quad (4)$$

Table 1 Haralick texture features (characteristics 1 to characteristics 22)

| S. no | Characteristics | S. no (continued) | Characteristics |
|-------|---------------------------------|----------------------|--------------------------------------|
| 1 | Contrast | 12 | Maximum probability |
| 2 | Correlation | 13 | Sum of squares |
| 3 | Energy/angular second moment | 14 | Sum average |
| 4 | Homogeneity | 15 | Sum variance |
| 5 | Autocorrelation | 16 | Sum entropy |
| 6 | Maximal correlation coefficient | 17 | Difference variance |
| 7 | Cluster prominence | 18 | Difference entropy |
| 8 | Cluster shade | 19 | Information measure of correlation 1 |
| 9 | Dissimilarity | 20 | Information measure of correlation 2 |
| 10 | Entropy | 21 | Inverse difference normalized |
| 11 | Homogeneity | 22 | Inverse difference moment normalized |

$$s_{x+y}(k) = \sum_{a=1}^N \sum_{b=1}^N s(a, b), \quad k = 1, 2, \dots, 2N \tag{5}$$

$$a + b = k$$

$$s_{x-y}(k) = \sum_{a=1}^N \sum_{b=1}^N s(a, b), \quad k = 0, 1, \dots, N - 1 \tag{6}$$

$$|a - b| = k$$

and $\mu_x, \mu_y, \sigma_x,$ and σ_y as the means and standard deviations of S_x and S_y , respectively. We used the [9] and [10] Haralick texture features with their equations (1–22) in Table 1.

3 Modeling Technique for SVM

Support vector machine (SVM) relies on the principle of structural risk decrease [11]. SVM learns associate degree best separating hyper plane from a given set of positive and negative examples. SVM are often used for pattern classification. For linearly severable knowledge, SVM finds a separating hyperplane that separates the information with the biggest margin. For linearly indivisible knowledge, it translates the information within the input area into a high-dimension area

$$x \in R^I \rightarrow \Phi(x) \in R^H \quad (7)$$

with kernel operate $\Phi(x)$, to find out the separating hyperplane. SVMs area unit evaluated as well-liked tools for learning from the given knowledge [12, 14]. The explanation is that, SVMs area unit is simpler than the normal pattern recognition approaches that supported the mix of a feature choice procedure and a standard classifier.

SVM is generally applied to linear margins. If a linear boundary is out of place, the SVM will map the input vector into a high dimensional feature area. Nonlinear mapping is selected by the SVM constructs to associate the best separating hyperplane in the higher dimensional area. A kernel function K is defined for generating the inner products to construct machines with different kinds of non-linear decision surfaces within the input area.

$$K(x, x_i) = \Phi(x) \cdot \Phi(x_i) \quad (8)$$

4 Experimental Results

4.1 Dataset

We evaluated the accuracy of our technique by acting experiments on information obtained as a part of the Parkinson's progression markers initiative (PPMI) (https://www.ida.loni.usc.edu/services/Menu/IdaData.jsp?page=DATA&subPage=AVAILABLE_DATA&project=PPMI). An outline of demographic and psychology details of subjects utilized in our study is bestowed in Table 2.

The database consists of 595 different data groups are available, which 32 are normal and 78 are PD.

4.2 Image Acquisition and Preprocessing

The structural $T2$ -weighted magnetization ready fast gradient echo images were nonheritable on a 1.5-T Vision scanner during an imaging period. From the original

Table 2 Clinical characteristics of PD patients and control subjects

| Total number of data characteristics | Control | With PD |
|--------------------------------------|------------|------------|
| MRI data (n) | 32 | 78 |
| Age | 45 ± 59 | 45 ± 69 |
| Sex (M/F) | 32 (17/15) | 78 (52/26) |
| Format | DCM | DCM |

image knowledge, the region of interest is fixed to a size of 95×95 . The ROI is fixed such that it provides enough information for feature selection. Image parameters: TR = 9.7 ms, TE = 4.0 ms, Flip angle = 10, TI = 20 ms, TD = 200 unit of time., 128 mesial 1.25 mm slices while not gaps and pixels resolution of 512×512 .

4.3 Feature Extraction

The features are extracted using Histogram and GLCM. Histogram is an image enhancement technique which normalizes gray level in the image. There are 8 histogram features and 22 GLCM features extracted from the image data which are combined to form a 30-dimensional feature vector. The cropped image is of size 95×95 . From the 120 MR images within the dataset, we have used 80 images for training and 40 pictures for testing. The training image set consists of 48 control images and 32 abnormal MR images. Within the training phase, the images are applied to the SVM which creates models numbered zero and one, 0 belong to Normal, 1 belong to PD. In the testing phase, the images are applied to the SVM which extracts the features from the images and creates models, these models are compared with the existing models to classify the image.

4.4 Modeling Using SVM

We use a nonlinear support vector machine modeling that is employed to classify the image. The 30 features that are extracted within the previous section are provided to SVM for model generation. The model generated by the SVM classifies the image information into traditional and Parkinson's sickness. The character of the dataset, total range of dataset used per class, and also the classification accuracy is bestowed in Table 3 (Figs. 1 and 2).

Table 3 Statistical parameters of classification accuracy

| Statistical parameters | Specificity | Sensitivity | Total classification accuracy |
|------------------------|---------------------------------------|---------------------------------------|------------------------------------|
| Accuracy | True +ve/ (True +ve) + (False -ve) | True -ve/ (False +ve) + (True -ve) | (True +ve) + (True -ve)/(P + N) |
| (%) | 83 | 89 | 87 |

Fig. 1 Control versus parkinson using SVM

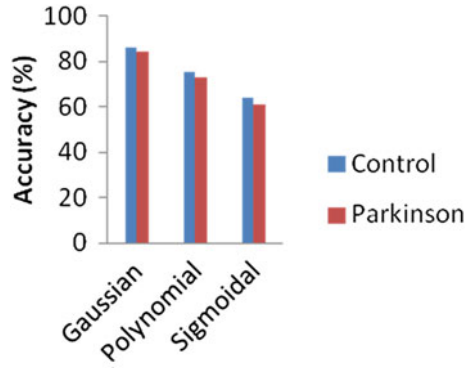
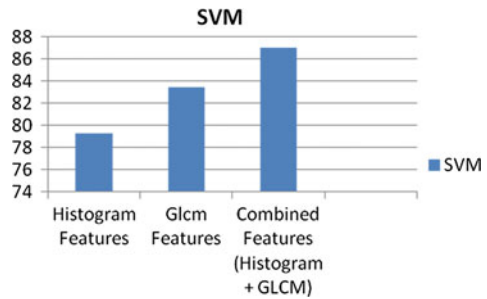


Fig. 2 Performance of classification for different combination of feature



5 Conclusions

In this paper, a system for classifying MRI image is described. ROI is manually calculated by cropping the MRI image. Histogram and GLCM features are extracted from the cropped image. 30 features are extracted from the ROI image. The features are given as input to the SVM for classification as Normal and PD. The experimental results show that the classification by SVM can produce a performance of accuracy, sensitivity, and specificity for the classifier (SVM). Measures could only be viewed on testing multiple images.

References

1. Pezard, L., Jech, R., Ruezlicika, E.: Investigation of non-linear properties of multichannel EEG in the early stages of Parkinson’s disease. *Clini Neurophysiol* **122**, 38–45 (2001)
2. Sakalauskas, A., Lukosevicius, A., Lauckaite, K., Jegelevicius, D., Rutkauskas, S.: Automated segmentation of transcranial sonographic images in the diagnostics of parkinson’s disease. *Elsevier—Ultrasonics*, **53**(1), 111–121 (2013)

3. Rana, B., Juneja, A., Saxena, M., Gudwani, S., Senthil Kumaran, S., Agrawal, R.K., Behari, M.: Regions-of-interest based automated diagnosis of Parkinson's disease using T1-weighted MRI. Elsevier—Expert Syst. Appl. **42**(9), 4506–4516 (2015)
4. Salvatore, C., Cerasa, A., Castiglioni, I., Gallivanone, F., Augimeri, A., Lopez, M., Arabia, G., Morelli, M., Gilard, M.C., Quattrone, A.: Machine learning on brain MRI data for differential diagnosis of Parkinson's disease and progressive supranuclear palsy. Elsevier—J. Neurosci. Methods **222**, 230–237, 30 Jan 2014
5. Gonzalez, R.C., Woods, R.E.: Digital Image Processing, 3rd edn. Prentice Hall, Upper Saddle River (2008)
6. Freeborough, P.A., Fox, N.C.: MR image texture analysis applied to the diagnosis and tracking of Alzheimer's disease. IEEE Trans. Med. Imaging **17**(3), June 1998
7. Haralick, R.M., Shanmugam, K.: Textural features for image classification. IEEE Trans. Syst. Man Cybern. **SMC-3**(6), Nov 1973
8. Soh, L.-K., Tsatsoulis, C.: Texture analysis of SAR sea ice imagery using gray level co-occurrence matrices. IEEE Trans. Geosci. Remote Sens. **37**(2), March 1999
9. Clausi, D.A.: An analysis of co-occurrence texture statistics using gray level co-occurrence matrices. Can. J. Remote Sens./J. Can. de Teledetect. **28**(1), 45–62 (2002)
10. Sarage, G.N., Sagar Jambhorkar, S.: Enhancement of mammography images for breast cancer detection using histogram processing techniques. IJCST **2**(4), 2011
11. Dhanalakshmi, P., Palanivel, S., Ramalingam, V.: Classification of audio signals using SVM and RBFNN. Elsevier, pp. 6069–6075 (2009)
12. Jing, H., Bai, J., Zhang, S., Xu, B.: SVM-based audio scene classification. In: Proceeding of IEEE, pp. 131–136 (2005)
13. Yegnanarayana, B., Kishore, S.P.: AANN: an alternative to GMM for pattern recognition. Neural Netw. **15**, 459–469 (2002)
14. Dhanalakshmi, P.: Classification of audio for retrieval applications. Ph.D. Thesis, Annamalai University (2010)